

Development of an optical fiber-based interferometer for strain measurements in non-destructive application

S. Pullteap¹ 

Received: 1 April 2016 / Accepted: 12 September 2016 / Published online: 19 September 2016
© Springer-Verlag Berlin Heidelberg 2016

Abstract In this paper, an extrinsic Fabry–Perot interferometer (EFPI) has been demonstrated for strain measurements. A monochromatic light source with a wavelength of 1310 nm is propagated into a single-mode fiber and then passed through the sensing arm. Approximately, 4 % of the beam is reflected off at the fiber end generating the “reference signal”, while the rest is next transmitted to the target and reflected back to the sensing arm as the “sensing beam”. The interference signal is, however, generated from the superposition between two beams (reference and sensing signals) in the fiber arm. The number of interference signal also called “fringe” is, normally, directly proportional to the displacement of the target movement. Fringe counting technique is also proposed for demodulating the fringe number to the displacement information. Consequently, the displacement is then converted to the strain value by referring to a basic of strain theory. A cantilever beam fastened to a mechanical wave driver has been utilized as a vibrator for the experimental studies. Two experiments have been investigated for the sensor performance’s study. By varying the frequency excitation from 60 to 180 Hz, and also the amplitude excitation from 0.25 to 5 V, the output strain range of 0.082–1.556 and 0.246–2.702 $\mu\epsilon$ has been apparent, respectively. In addition, a commercial strain sensor has also been used as a reference, leading to an average percentage error of 1.563 %.

Keywords Fabry–Perot interferometer · Interference signal · Non-destructive measurement · Strain measurement

1 Introduction

Nowadays, many types of the industrial materials such as concrete, steel rod, stainless steel and aluminum have been used as material part for the infrastructure construction (i.e., house, building, bridge, dam, etc.). It has several advantages over the wood constructions such as robust to the environmental effects, corrosion resistant and ductility [1,2]. However, the material fatigue or cracking due to gross error, environmental effects and long-time usages is the main effect of these materials. Temperature change, vibration, earthquake, and storm are examples of the effects of the environment. To investigate these effects, the high-precision detectors, such as displacement sensor, seismometer and capacitive sensor, have been offered for monitoring the problems. Fiber optic sensor (FOS) is also a type of the measuring instrument that has often been applied for analyzing such problem. Several advantages over the electronic instruments such as immunity to electromagnetic wave, possibility to work on the hazardous areas, small size and lightweight [3–5] makes FOS a well-known detection system for measuring the environmental effects. In general, the sensor can be separated into various categories. Fiber optic interferometers (FOIs) are an example of the sensor which can, additionally, be classified into four main types: Michelson, Mach–Zehnder, Sagnac, and Fabry–Perot, respectively. Several mechatronic engineering applications used these interferometers for high-precision measurements. For example, Dorband et al. explained the operation of Michelson fiber interferometer (MFI) for several engineering applications with a high sensitivity [6]. In addition, a ring Mach–Zehnder interferometer for vibration measurement with a dynamic range of 38 meters was demonstrated by Qizhen et al. [7]. Furthermore, a study of the polarization-maintaining photonic crystal fiber (PM-PCF) based on Sagnac interferometer

✉ S. Pullteap
saroj@su.ac.th

¹ Department of Mechanical Engineering, Faculty of Engineering and Industrial Technology, Silpakorn University (Sanam Chandra Palace), Nakhon Pathom, Thailand

was demonstrated by Fu et al. [8] for the pressure measurements. This fiber interferometer had a capability to detect a small pressure from the material or target with a sensitivity of 3.42 nm/MPa. In terms of Fabry–Perot interferometer, Pullteap et al. [9], however, developed an extrinsic fiber-based Fabry–Perot interferometer (EFFPI) for high-precision displacement measurements in various excitation waveforms. The fiber optic interferometer could, extremely, detect the displacement range of 0.7–140 nm without directional ambiguity.

In recent work, a fiber-based Fabry–Perot interferometer was proposed for small displacement measurement in the range of 0.65–15.06 μm with a resolution of $\lambda/2$ [10]. In this work, the developed sensor has, continuously, been applied for strain measurement study. An aluminum plate screwed to the mechanical vibrator has thus been proposed as a cantilever beam for the strain investigation. By specifying the excitation frequency and excitation amplitude from a classical function generator to the vibrator, the strain information due to material vibration has been generated. This quantity is proportional to a dynamic displacement range, which is obtained from the fiber sensor via a fringe counting demodulation technique. Moreover, an electrical strain sensor has been utilized as a reference sensor for investigating the errors and also the sensor performance. The designed system might, consequently, be applied either to mechatronic engineering applications or the non-destructive measurements, respectively.

2 Principles of strain measurements using fiber optic interferometers

2.1 Classification of fiber interferometers

Fiber optic interferometers were popular high-precision instruments that were first developed more than three decade ago [11–13]. As mentioned in the previous section, there are four categories of the fiber optic-based interferometers, the configurations of which are shown in Fig. 1. Basically, the interferometers have been operated on the light intensity change or phase shift between two considered beams, sensing and reference beams, leading to the occurrence of interferogram pattern. This signal is then decoded to the physical quantities such as displacement, temperature, stress and acoustic wave [14–16]. Consequently, we could observe that several engineering and scientific applications used the sensor for the precision measurements [17–19].

The operating principles of the fiber optic-based Michelson and Mach–Zehnder interferometers have been described in Fig. 1a, b. The beam from a light source has, first, been propagated through a fiber coupler and then separated (50:50) into two beams; one is passed through to the reference arm

called “reference signal”, while the other is injected along the sensing arms as a “sensing signal”. The signals are then superposed on each other at the output arms, leading to the formation of interference signal.

In addition, the fiber-based Sagnac interferometer has been shown in Fig. 1c. The light beam from a laser source is, first, injected into a single-mode (SM) fiber and then passed through a polarizer for separating the orthogonal components of the light (vertical and horizontal polarization beams). This light is, next, spitted into two beams (50:50) using a fiber coupler and propagated into a fiber coiled. The first path of the propagated beam is rotated clockwise, while the other is counterclockwise, respectively. The path difference between two directional beams is pointed to an angular speed (Ω) which is, normally, related to the physical quantity of the target. The fiber-based Fabry–Perot interferometer (FFPI) is, however, a latter type of the FOIs which configuration is shown in Fig. 1d. A monochromatic light from the laser source is propagated through a 50/50 fiber coupler to the sensing arm. Approximately, 4 % of the light is reflected off at the fiber end as a “reference signal”, while a 96 % of the light is transmitted to the target and reflected back to the fiber cave end as a “sensing signal”, respectively. Consequently, the interference signal is generated by the superposition between two beams and then passed to the output fiber arm. However, the advantage of the FFPI configuration over the other interferometers is using only single arm, but a double cavity can be found [14]. Consequently, it is economized for the optical device insertion and simple to develop.

In this work, a development of an extrinsic fiber-based Fabry–Perot interferometry (EFPI) has been proposed for strain measurements in a target material. Basically, it is operated based on intensity demodulation. The inference signal or “fringe” has, however, been focused for signal demodulation to the desired measurand [14]. The intensity of the fringe signal (I) detected by a photodetector can, thus, be given by:

$$I = I_r + I_s + 2\sqrt{I_r I_s} \cos \Delta\phi \quad (1)$$

where I_r corresponds to the output intensity of reference signal detected by the photodetector, while I_s is an output intensity of the sensing signal, respectively. Consequently, the phase difference between two beams (ϕ_r and ϕ_s) can be denoted as $\Delta\phi$. It is, normally, related to the cavity length or optical path length between the fiber end and desired target which can be written by:

$$\Delta\phi = \frac{2\pi n}{\lambda} 2d \quad (2)$$

where n is the refractive index ($n = 1$ for the air), λ is the wavelength of light source and d is the displacement length between fiber end and target.

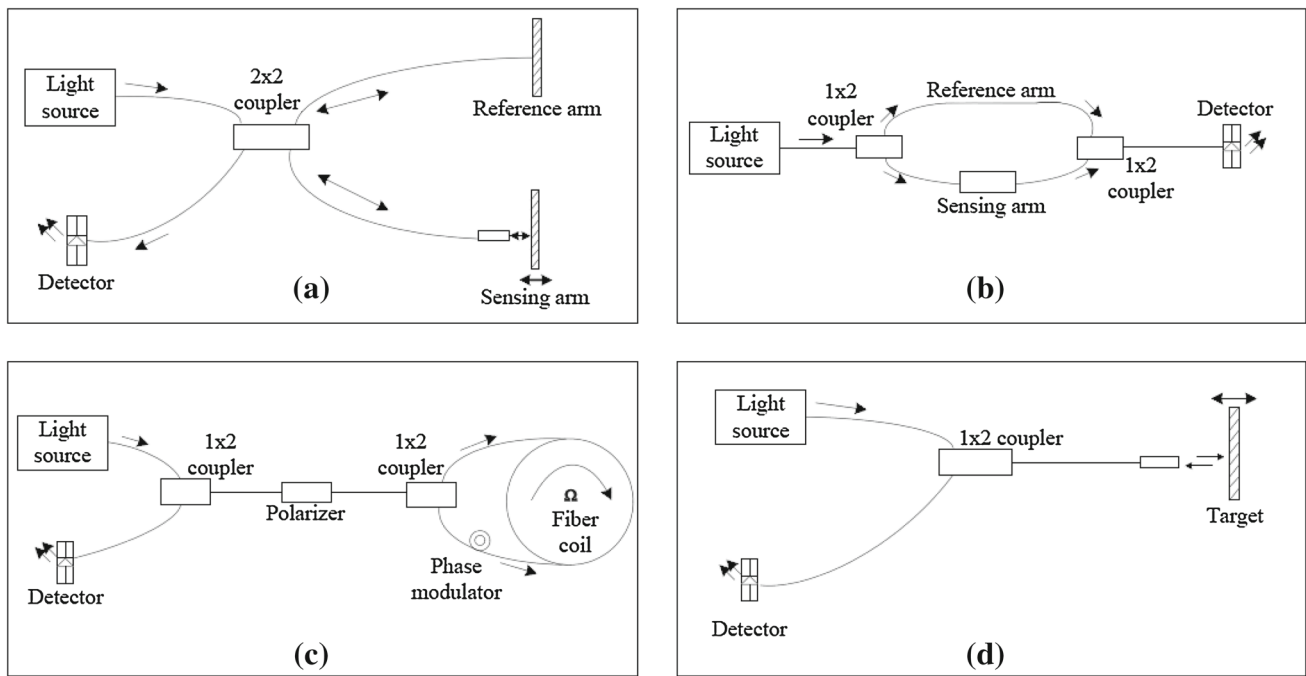


Fig. 1 Configurations of fiber optic-based interferometers: **a** Michelson interferometer, **b** Mach–Zehnder interferometer, **c** Sagnac interferometer, **d** Fabry–Perot interferometer

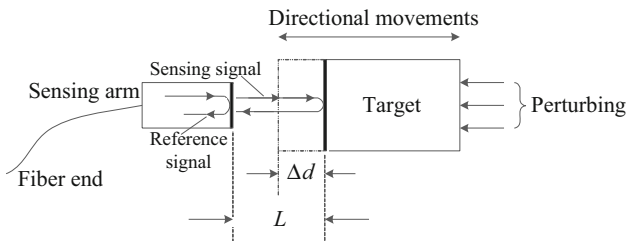


Fig. 2 Strain measurement concepts using EFPI sensor

Further, the number of fringe (N) is, generally, directly proportional to the displacement of the target movement (d) which can thus be calculated by:

$$d = N \times \frac{\lambda}{2} \tag{3}$$

To obtain the strain information, the fiber-based EFPI’s configuration has thus been focused, concepts of which are illustrated in Fig. 2.

Considering to the figure, the distance between the target and sensing arm of the fiber interferometer is defined by L . However, this value can be changed by Δd when the specimen has been perturbed either in horizontal or vertical directions, leading to the optical path length transformed. This phenomenon is, however, related to the number of fringe change that is obtained from the sensor. In addition, the strain

value (ε) has been found using the following equation [2]:

$$\varepsilon = \frac{\Delta d}{L} \tag{4}$$

where Δd corresponds to the changing of cavity length, while L corresponds to the cavity length between the sensing arm and the target, respectively.

Furthermore, the fiber optic interferometers for strain measurements were also considered in several applications. For example, Udd reported the smart structures by utilizing the FOSs for investigating the strain information of the bridges [4]. Moreover, Habel et al. also described the capability of an extrinsic Fabry–Perot interferometer (EFPI) and the distributed fiber sensor for several geotechnical engineering applications [20]. Consequently, the fiber-based Mach–Zehnder interferometer for the dynamic strain measurement applications was also designed and demonstrated by Her et al. [21].

2.2 Principles of strain measurement

Basically, the strain information is typical of the physical quantity which was caused due to the deformation of material specimen due to any applied forces (F) to the desired material such as tensile or compression forces. Moreover, it has also been correlated to the difference length (ΔL) of the material specimen after forcing either in perpendicular or longitudinal directions, as the basic principle shown in Fig. 3.

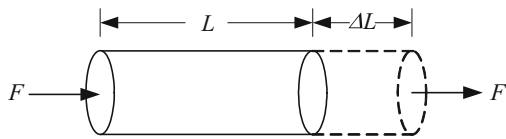


Fig. 3 Basic principle of strain phenomena

Furthermore, a basic strain equation has been indicated below:

$$\varepsilon = \frac{\Delta L}{L} \quad (5)$$

where ε is the axial strain, L is the initial length of material specimen and ΔL is the difference length of specimen.

To obtain the strain value, several measuring instruments have been proposed such as electrical strain gauges, mechanical extensometers, and also optical extensometers [22]. According to first instrument, the strain information can be found in terms of the resistance change due to the forcing of the copper or iron wire inside the device. This value is then connected to a classical Wheatstone bridge circuit for transforming the resistance value to electrical quantity and then passed through the signal conditioning circuit for demodulation of the signal to the strain information, respectively. Moreover, the electrical strain gauge is widely used for strain measurements in several engineering applications due to simplicity of the installation and usage, economic price, ease of compensation for the temperature and humidity effects, etc. [22].

Mechanical extensometer is another type of the strain instrument that has been used for studying the material properties [23]. The main advantages of this instrument are simplicity to utilize and ability to read analog data. However, it is a contact instrument in which the instrument probe (knife edge) has been touched to the surface specimen directly. Therefore, the strain information depends on the surface roughness of the specimen. However, it has been limited to the sensitivity, and also the specimen surface might be destructed due to instrument probe contacting. To eliminate these effects, the optical extensometer has, however, been proposed for strain investigation. It is a non-contact measuring instrument, in which the specimen's surface has never been destructed from the instrument probe. Consequently, this instrument is operated on the principle of optical path length change due to any forces (tensile or compression) to the material. Moreover, the optical extensometer is extremely sensitive than the mechanical extensometer and also the strain gauges. However, it is more complicated to use and implement (due to installation of the bulk optical devices inside), and also highly priced, leading to its use only in the laboratory of science and engineering for non-contact measurement applications [23].

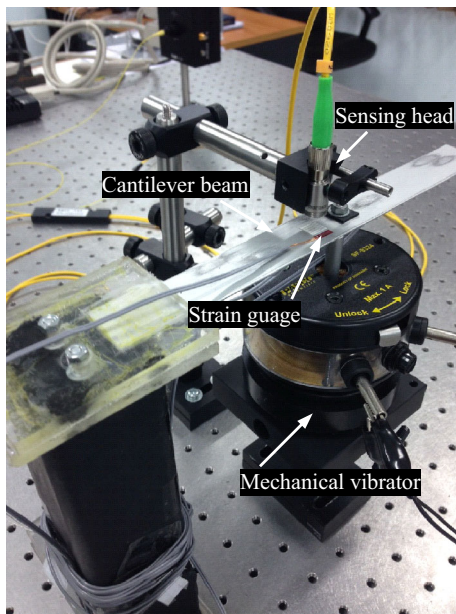
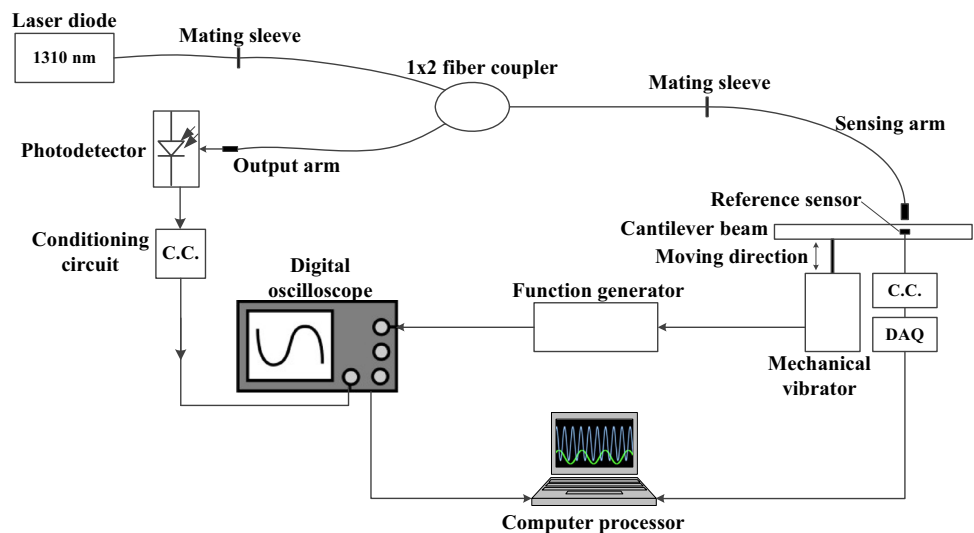
In this work, the fiber-based EFPI has, however, been developed as an optical extensometer for strain measurements with several advantages over the classical extensometer such as low cost, easy to use, and also simplicity to implement. Its sensor structure uses only some optical components. Therefore, effects due to optical misalignment can be eliminated (see Fig. 1d). Therefore, some effects of from the optical misalignment can thus be eliminated. In addition, more advantages of the optical fiber-based Fabry–Perot interferometer over the commercial sensors can be summarized in terms of high sensitivity, wide range and bandwidth, capability to embed into constructions, etc. [4–8].

3 Experimental setup

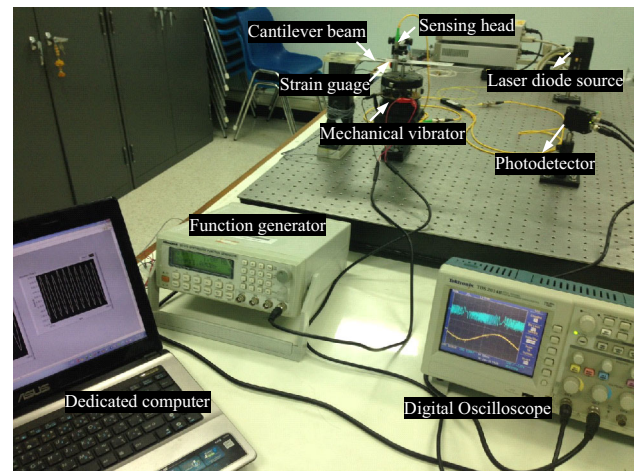
The configuration of extrinsic fiber Fabry–Perot interferometer for strain measurements has, consequently, been illustrated in Fig. 4.

According to Fig. 4, the experiment has been demonstrated on an optical table without controlling room temperature. A monochromatic light with a wavelength of 1310 nm by Thorlabs Inc. has been used as a laser diode source. This beam is, next, propagated into a single-mode fiber (SMF-28), and then passed through a 1×2 fiber coupler to the sensing arm of the fiber sensor via the mating sleeves. There is approximately 4 % of the light reflected back from the fiber caved end as a “reference signal”, while the rest is transmitted to the target. Consequently, a “sensing signal” is then generated, when the transmission beam from the cantilever beam (target) is reflected back to the fiber arm. Furthermore, the interference signal from two indicated beams has thus been formed due to the superposition phenomena in the fiber arm. This signal is next passed to the output arm and then converted to the electrical quantity (in voltage) using a photodetector. The output signal is consequently arranged using a signal conditioning circuit (CC), before sending to a digital oscilloscope for displaying the interference waveform. In addition, a commercial strain gauge from Tokyo Sokki Kenkyujo Ltd. model: FLA-1-11 has also been attached to the cantilever beam near the sensing head position of the fiber sensor as a “reference sensor”. The installation has been illustrated in Fig. 5.

By varying the excitation frequency from 60 to 180 Hz, but fixing excitation amplitude of 250 mV from the Pasco Mechanical Wave Driver model SF-9324 that is installed on the optical table, the interference signal has been found on the oscilloscope. Consequently, the number of interferogram data (or fringe) has been demodulated using the fringe counting technique, and then this information is transferred to a dedicated computer for data signal processing. Generally, these data are correlated to the displacement of target movement as shown in Eq. (3). Moreover, the strain infor-

Fig. 4 Configuration of EFPI sensor for strain measurements**Fig. 5** Installation of EFPI and strain gauge on cantilever beam

mation has also been found by referring to (4) cooperating with a demodulated program that is developed by MATLAB programming. Further, the output data from the reference sensor have been transferred to an electronic data acquisition system (DAQ) model: EMANT300, and next interfaced to the computer for signal processing using Labview programming. Consequently, the dynamic strain information has been found as a “reference data” from the system. By comparing the experimental result as detected from the fiber sensor and reference sensor, the measurement error has, thus, been reported. This information would indicate the performance of the fiber interferometer for applications in the non-destructive or high-precision measurements.

**Fig. 6** Experimental setup of EFPI for strain measurements

4 Experimental results and discussion

According to the experiment procedures as described in the previous section, the configuration of the extrinsic fiber Fabry–Perot interferometer for the strain investigations has, consequently, been illustrated in Fig. 6. In addition, we choose the sinusoidal waveform (with an excitation frequency of 70 Hz and 250 mV for excitation amplitude) from a function generator to drive the mechanical vibrator for the preliminary study. However, the output interference signal detected by a photodetector has been illustrated in Fig. 7.

In Fig. 7, the number of interference signal has thus been found for 5 fringes. It implies that a displacement information of $3.875 \mu\text{m}$ is indicated, which is also correlated to a strain value of $0.484 \mu\epsilon$, respectively. Consequently, the strain value from the reference sensor has been obtained as $0.485 \mu\epsilon$, its results is shown in Fig. 8.

According to the experimental results from the Figs. 7 and 8, we can summarize that a percentage error of 0.206 % has, thus, been indicated from the measurement system. However, this value might be generated either from the systematic or gross errors. In addition, the experimental results by varying the excitation frequency in the range of 60–180 Hz, but fixing the excitation amplitude of 250 mV has, consequently, been reported in Fig. 9.

According to the Fig. 9, we can conclude that a maximum strain value obtained by the EFPI sensor (at the excitation

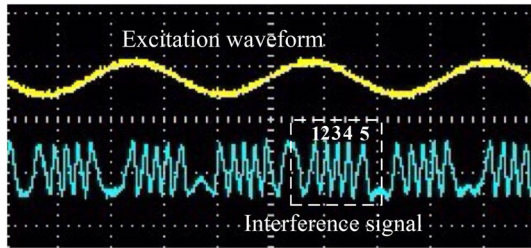


Fig. 7 An experimental result using excitation frequency of 70 Hz, and excitation amplitude of 250 mV

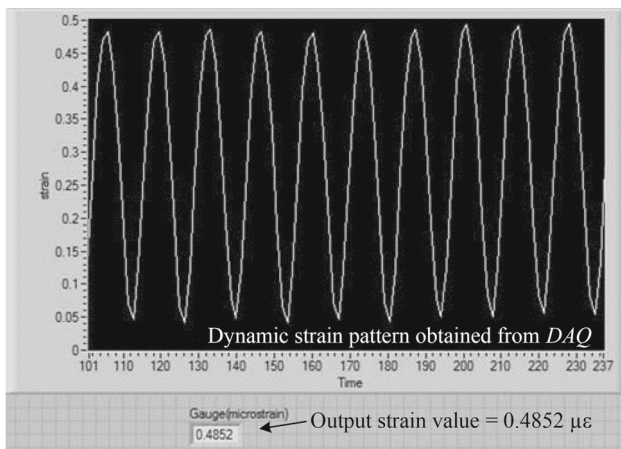
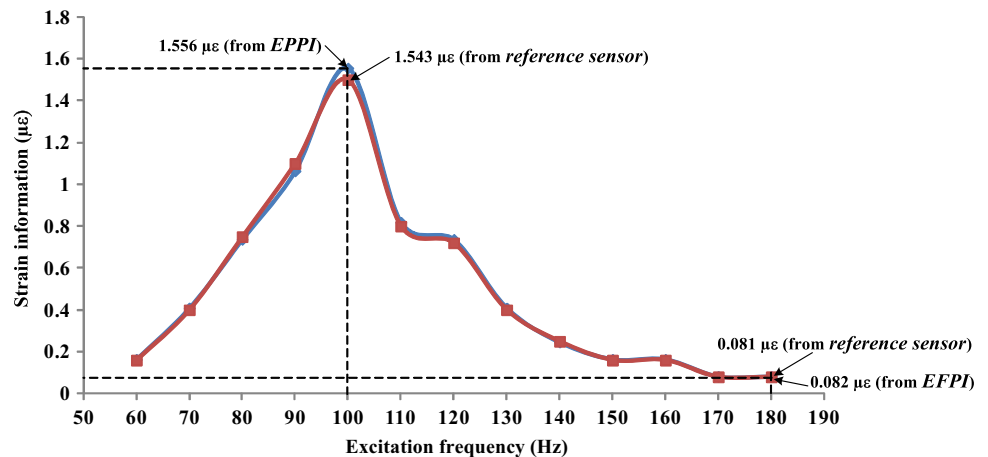


Fig. 8 Output strain value obtained by reference sensor

Fig. 9 Output strain information measured by EFPI compared with reference sensor at 250 mV for excitation amplitude



frequency of 100 Hz) has been 1.556 $\mu\epsilon$, while for reference sensor is 1.543 $\mu\epsilon$. This corresponds to the resonance frequency of the mechanical vibrator. In addition, a minimum strain from both sensors has been 0.081 $\mu\epsilon$ by the reference sensor, and 0.082 $\mu\epsilon$ by the fiber sensor. By repeating the measured results of 5 times/each, the percentage errors such as the minimum, maximum, and average have been studied. These results can be summarized in Fig 10.

As illustrated in Fig. 10, we report that a minimum, maximum, and also average measurement error have continuously been found to be 0.183, 2.537, and 1.563 %, respectively. These values are validating the performance of the fiber sensor for strain investigations with small errors due to some important factors such as temperature changes from the environmental effect, target position instability, surrounding forced vibration from the external environments, gross error and electronic drift. In addition, the small error might be generated from the installation of the sensing head close to the reference sensor. Therefore, the effects from those problems have also been reflected on the strain gauges. This implies that the output from the EFPI sensor is directly proportional to the output from strain gauges. To verify the sensor’s performance, another experiment has, consequently, been studied. By fixing the frequency excitation of 60 Hz and varying the amplitude excitation from 0.25 to 5 V (upper excitation limit of a mechanical vibrator), the output strain information range measured by the EFPI sensor is indicated from 0.246 to 2.702 $\mu\epsilon$, while the reference sensor is 0.250–2.654 $\mu\epsilon$, respectively, leading to an average error of 1.782 %. The results have been detailed in Fig. 11.

It implies that the output strain values are directly proportional to the variation of amplitude excitation. However, we might give an explanation about this phenomenon using a classical equation of the Newton law’s. Assume that a value of the target mass (m) is fixed, while the variation of target force (F) corresponds to the amplitude excitation on the mechanical vibrator. Consequently, the target displacement is correlated to the target acceleration (a). Therefore, the

Fig. 10 Percentage errors obtained from experiment

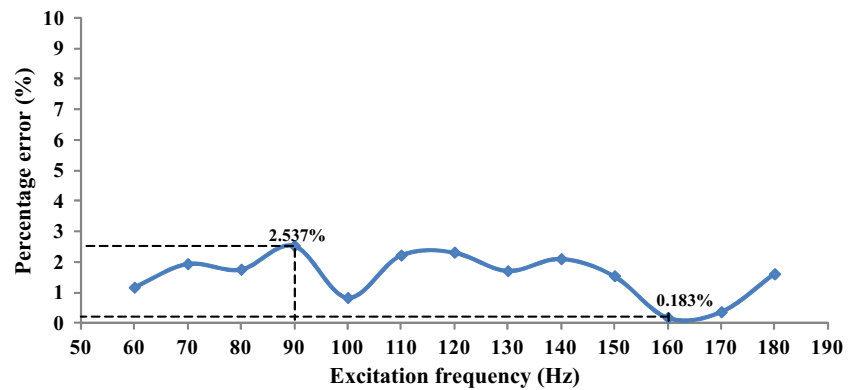
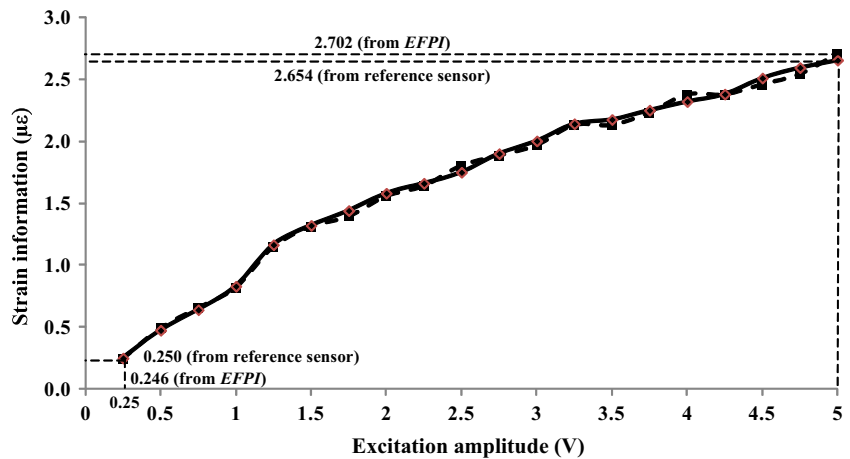


Fig. 11 Experimental validation by varying amplitude excitation from 0.25–5 V



target displacement variation (Δd) is, absolutely, related to the target force, which is also involved in the experimental results shown in Fig. 11. Furthermore, the strain information will grow up when the excitation amplitude is increased. In addition, the errors might be found due to several factors that have already been mentioned in the previous sections. To reduce those errors, we have to concentrate on the environmental effects and also gross errors such as room temperature and humidity controlling, avoiding demonstration when the environmental vibration occurred, setting up the experiment properly and using a precise instruments to measure the data.

Last but not least, two experimental results above could, however, verify that the EFPI sensor which is highly sensitive has been applied for strain measurements. Moreover, the fiber sensor can also be operated on the non-contact measurement, in which the target surface is never destroyed from the sensing probe. Therefore, we can clarify that the EFPI sensor has the ability to be used in non-destructive measurements.

5 Conclusion

An extrinsic fiber Fabry–Perot interferometer (EFPI) has been developed for the dynamic strain measurements. A cantilever beam fastened to the mechanical vibrator has been

used as a vibrating target. By forcing the cantilever beam with the excitation frequency range of 60–80 Hz, the strain values of 0.082–1.556 $\mu\epsilon$ were obtained, while an average error of 1.563 % was reported by comparing the results with the commercial strain sensor. To verify the sensor performance, another experiment was proposed. By varying the amplitude excitation from 250 mV to 5 V, the output strain was found to be 0.246–2.702 $\mu\epsilon$, while the average error was also 1.782 % respectively. The experimental results could thus show that the EFPI sensor was better performing for high-precision measurements either in mechatronics engineering or non-destructive measurement applications.

Acknowledgements This research was a funding supported by the National Science and Technology Development Agency (NSTDA), Thailand.

References

1. Ashby M, Shercliff H, Cebon D (2014) Material engineering, science, processing and design. Elsevier, UK
2. Mukhopadhyay SC, Jayasundra KP, Funchs A (2013) Advancement in sensing technology: new developments and development applications. Springer-Verlag, Berlin, Heidelberg

3. Antune P, Lim H, Varum H, André P (2012) Optical fiber sensors for static and dynamic health monitoring of civil engineering infrastructures: abode wall case study. *Measurement* 45:1695–1705
4. Udd E (1991) *Fiber optic sensor: an introduction for engineers and scientists*. Wiley, New York
5. Grattan KTV, Meggitt BT (1998) *Optical fiber sensor technology: devices and technology*. Chapman & Hall, London
6. Dornband B, Muller H, Gross H (2012) *Handbook of optical systems*. Wiley-VCH Verlag GmbH & Co KGaA, Germany
7. Sun Q, Liu D, Wang J, Liu H (2008) Distributed fiber-optic vibration sensor using a ring Mach-Zehnder interferometer. *J Opt Commun* 281:1538–1544
8. Santos JL, Farahi F (2015) *Handbook of optical sensors*. CRC Press, New York
9. Pullteap S, Seat H (2015) An extrinsic fiber fabry-perot interferometer for dynamic displacement measurement. *Photonic Sens* 5–1:50–59
10. Pullteap S (2012) Development of an optical fiber based interferometer for small vibration measurements. In: *IEEE International conference on optical communications and networks (ICOON)*, pp 107–110
11. Udd E, Spillman WB (2011) *Fiber optic sensors: an introduction for engineers and scientist*. Wiley, New Jersey
12. Gåsvik KJ (2002) *Optical metrology*. Wiley, London
13. Udd E (2006) *Fiber optic sensors: an introduction to for engineers and scientists*. Wiley, New Jersey
14. Hernandez G (1986) *Fabry-Perot interferometers*. Cambridge University Press, Cambridge
15. Mihailov SJ (2012) Fiber Bragg grating sensors for harsh environments. *Sensors* 12:1898–1918
16. Sun H, Yang S, Zhang X, Yuan L, Yang Z, Hu M (2015) Simultaneous measurement of temperature and strain or temperature and curvature based on an optical fiber Mach-Zehnder interferometer. *Opt Commun* 340:39–43
17. Bravo M, Pinto AMR, Lopez-Amo M, Kobelke J, Schuster K (2012) High precision micro-displacement fiber sensor through a suspended-core Sagnac interferometer. *Opt Lett* 2:202–204
18. Lee BH, Kim YH, Park KS, Eom JB, Kim MJ, Rho BS, Choi HY (2012) Interferometric fiber optic sensors. *Sensors* 12:2467–2486
19. Li Lecheng, Xia Li, Xie Zhenhai, Liu Deming (2012) All-fiber Mach-Zehnder interferometers for sensing applications. *Opt Exp* 20:11109–11120
20. Habel WR, Krebber K (2011) Fiber-optic sensor applications in civil and geotechnical engineering. *Photonic Sens* 1:268–280
21. Her SC, Huang CY (2011) Effect of coating on the strain transfer of optical fiber sensors. *Sensors* 11:6926–6941
22. Figliola RS, Beasley D (2015) *Theory and design for mechanical measurements*. Willey, USA
23. Ye L, Feng P, Yue Q (2011) *Advances in FRP composites in civil engineering*. Tsinghua University Press, Beijing